Environ. Sci. Technol. **2002**, *36,* 2395−2402

Atmospheric Chemistry of HFE-7500 [n-$C_3F_7CF(OC_2H_5)CF(CF_3)_2$]: Reaction with OH Radicals and Cl Atoms and Atmospheric Fate of n-$C_3F_7CF(OCHO\bullet)CF(CF_3)_2$ and n-$C_3F_7CF(OCH_2CH_2O\bullet)CF(CF_3)_2$ Radicals

M. GOTO, Y. INOUE, AND M. KAWASAKI

Department of Molecular Engineering, Kyoto University, Kyoto 606-8501, Japan

A. G. GUSCHIN, L. T. MOLINA, AND M. J. MOLINA

Department of Earth, Atmospheric, and Planetary Sciences, Massachusetts Institute of Technology, Cambridge, Massachusetts 02139

T. J. WALLINGTON* AND M. D. HURLEY

Ford Research Laboratory,SRL-3083, Ford Motor Company, P.O. Box 2053, Dearborn, Michigan 48121-2053

Relative rate techniques were used to measure k(OH + HFE-7500) = (2.6 ± 0.6) × 10^{-14}, k(Cl + HFE-7500) = (2.3 ± 0.7) × 10^{-12}, k[Cl + n-$C_3F_7CF(OC(O)H)CF(CF_3)_2$] = (9.7 ± 1.4) × 10^{-15}, and k[Cl + n-$C_3F_7CF(OC(O)CH_3)CF(CF_3)_2$] < 6 × 10^{-17} cm^3 molecule^{-1} s^{-1} at 295 K [HFE-7500 = n-$C_3F_7CF(OC_2H_5)CF(CF_3)_2$]. From the value of k(OH + HFE-7500) an estimate of 2.2 years for the atmospheric lifetime of HFE-7500 is obtained. Two competing loss mechanisms for n-$C_3F_7CF(OCHO\bullet CH_3)CF(CF_3)_2$ radicals were identified in 700 Torr of N_2/O_2 diluent at 295 K; reaction with O_2 and decomposition via C−C bond scission with k_{O_2}/k_{decomp} = 0.013 ± 0.006 Torr^{-1}. The Cl atom initiated oxidation of HFE-7500 in N_2/O_2 diluent gives n-$C_3F_7CF(OC(O)CH_3)CF(CF_3)_2$ as the major product and n-$C_3F_7CF(OC(O)H)CF(CF_3)_2$ as a minor product. The atmospheric oxidation of HFE-7500 gives n-$C_3F_7CF(OC(O)CH_3)CF(CF_3)_2$ and n-$C_3F_7CF(OC(O)H)CF(CF_3)_2$ as oxidation products. The results are discussed with respect to the atmospheric chemistry and environmental impact of HFE-7500.

1. Introduction

Recognition of the adverse environmental impact of chlorofluorocarbon (CFC) release into the atmosphere (*1*, *2*) has led to an international effort to replace CFCs with environmentally acceptable alternatives. Hydrofluoroethers (HFEs) are a class of fluid compounds that have been developed to replace CFCs in applications such as the cleaning of electronic equipment, heat transfer agents, and carrier fluids for lubricant deposition (*3*). HFE-7000 (n-$C_3F_7OCH_3$), HFE-7100 [supplied commercially as a mixture of 35% n-$C_4F_9OCH_3$ and 65% $(CF_3)_2CFCF_2OCH_3$], and HFE-7200 [supplied commercially as a mixture of 35% n-$C_4F_9OC_2H_5$ and 65% $(CF_3)_2CFCF_2OC_2H_5$] have attracted commercial interest and we have reported assessments of their atmospheric chemistry (*4*−*6*). HFE-7500 [n-$C_3F_7CF(OC_2H_5)CF(CF_3)_2$, 2-trifluoromethyl-3-ethoxydodecafluorohexane] is a new member of this class of compounds. HFE-7500 is a volatile liquid (bp 130 °C) with a vapor pressure of 16 Torr at 25 °C (*7*) and will probably be released into the atmosphere. Prior to its large-scale industrial use, an assessment of the atmospheric chemistry, and hence environmental impact, of HFE-7500 is needed. We report the results of the first study of the atmospheric chemistry of HFE-7500.

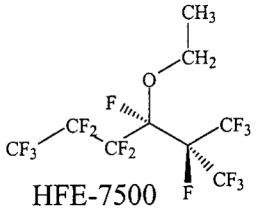

HFE-7500

The atmospheric oxidation of HFE-7500 will be initiated by reaction with OH radicals. The alkyl radicals produced in reaction 1 will add O_2 rapidly to give peroxy radicals:

$$n\text{-}C_3F_7CF(OCH_2CH_3)CF(CF_3)_2 + OH \rightarrow n\text{-}C_3F_7CF(OCH\bullet CH_3)CF(CF_3)_2 + H_2O \quad (1a)$$

$$n\text{-}C_3F_7CF(OCH_2CH_3)CF(CF_3)_2 + OH \rightarrow n\text{-}C_3F_7CF(OCH_2CH_2\bullet)CF(CF_3)_2 + H_2O \quad (1b)$$

$$n\text{-}C_3F_7CF(OCH\bullet CH_3)CF(CF_3)_2 + O_2 + M \rightarrow n\text{-}C_3F_7CF(OCHOO\bullet CH_3)CF(CF_3)_2 + M \quad (2a)$$

$$n\text{-}C_3F_7CF(OCH_2CH_2\bullet)CF(CF_3)_2 + O_2 + M \rightarrow n\text{-}C_3F_7CF(OCH_2CH_2OO\bullet)CF(CF_3)_2 + M \quad (2b)$$

The peroxy radicals derived from HFE-7500 will react with NO, NO_2, HO_2, and other peroxy radicals in the atmosphere (*8*, *9*):

$$n\text{-}C_3F_7CF(OC_2H_4OO\bullet)CF(CF_3)_2 + NO \rightarrow n\text{-}C_3F_7CF(OC_2H_4O\bullet)CF(CF_3)_2 + NO_2 \quad (3a)$$

$$n\text{-}C_3F_7CF(OC_2H_4OO\bullet)CF(CF_3)_2 + NO + M \rightarrow n\text{-}C_3F_7CF(OC_2H_4ONO_2)CF(CF_3)_2 + M \quad (3b)$$

$$n\text{-}C_3F_7CF(OC_2H_4OO\bullet)CF(CF_3)_2 + NO_2 + M \rightarrow n\text{-}C_3F_7CF(OC_2H_4O_2NO_2)CF(CF_3)_2 + M \quad (4)$$

$$C_3F_7CF(OC_2H_4OO\bullet)CF(CF_3)_2 + HO_2 \rightarrow \text{products} \quad (5)$$

$$C_3F_7CF(OC_2H_4OO\bullet)CF(CF_3)_2 + R'O_2 \rightarrow \text{products} \quad (6)$$

Experiments have been performed in our laboratories to elucidate the atmospheric chemistry of HFE-7500. A relative rate method was used at MIT to measure the kinetics of the reaction of OH radicals with HFE-7500 and hence to provide an assessment of its atmospheric lifetime. Relative rate methods were used at Ford to measure the kinetics of the reaction of Cl atoms with HFE-7500 and its oxidation products. Fourier transform infrared (FTIR) spectroscopy coupled to a smog chamber at Ford was employed to

* Corresponding author phone: [redacted]; fax: [redacted]; e-mail: [redacted]@ford.com.

10.1021/es0113798 CCC: $22.00
Published on Web 04/25/2002

investigate the atmospheric fate of the alkoxy radicals $C_3F_7CF(OCHO\bullet CH_3)CF(CF_3)_2$ and $C_3F_7CF(OCH_2CH_2O\bullet)CF(CF_3)_2$. The results are reported herein and discussed with respect to the environmental impact of HFE-7500.

2. Experimental Section

The two experimental systems used are described in detail elsewhere (*10*, *11*). All samples of HFE-7500 used in this work were supplied by the 3M Company at a purity >99% and were used without further purification. The uncertainties reported in this paper are two standard deviations unless otherwise stated. Standard error propagation methods were used to combine uncertainties where appropriate.

2.1. FTIR−Photolysis System at MIT. The rate constant for the OH + HFE-7500 reaction was obtained by monitoring the disappearance rate of HFE-7500 relative to CH_4 and CH_3Cl in the presence of OH radicals at 295 K. The decay of the sample was measured by infrared spectroscopy (*10*). The concentration of HFE-7500 was monitored by spectral subtraction. OH radicals were generated by photolysis of ozone at 254 nm in the presence of water vapor:

$$O_3 + h\nu \rightarrow O(^1D) + O_2 \quad (7)$$

$$O(^1D) + H_2O \rightarrow 2OH \quad (8)$$

The long-path absorption cell, made of Pyrex glass, had a volume of 7.6 L and a base length of 60 cm, which was adjusted to give a total of 24 passes and an optical path length of 14.4 m. The concentrations of the reactants and products were monitored with an FTIR spectrometer (Nicolet 20SX). The mercury photolysis lamp (Ace Hanovia 450-Watt medium-pressure mercury lamp) was enveloped in a Vycor tube, which transmits 254-nm radiation but absorbs the 185-nm Hg line, and was placed inside the absorption cell. No decay of the HFE-7500 sample was observed upon irradiation in the chamber in the absence of ozone.

The organic reactants were mixed with helium in a 3-L glass reservoir to yield mole fractions of ~1%. Ozone was prepared by first trapping the effluent from an ozonizer in cold silica gel, and then desorbing the sample into a 12-L glass reservoir and subsequently mixing it with helium. The experiments were performed at room temperature in ~200 Torr of helium as a buffer gas in the presence of 3−5 Torr of ozone and 2−3 Torr of water vapor.

2.2. FTIR−Smog Chamber System at Ford Motor Company. Experiments were performed in a 140-L Pyrex reactor interfaced to a Mattson Sirus 100 FTIR spectrometer (*11*). The reactor was surrounded by 22 fluorescent blacklamps (GE F15T8-BL), which were used to photochemically initiate the experiments. The oxidation of HFE-7500 was initiated by reaction with Cl atoms, which were generated by the photolysis of molecular chlorine in air diluent at 700 Torr total pressure at 295 ± 2 K.

$$Cl_2 + h\nu \rightarrow 2Cl \quad (9)$$

$$Cl + n\text{-}C_3F_7CF(OC_2H_5)CF(CF_3)_2 \rightarrow n\text{-}C_3F_7CF(OC_2H_4\bullet)CF(CF_3)_2 + HCl \quad (10)$$

$$n\text{-}C_3F_7CF(OC_2H_4\bullet)CF(CF_3)_2 + O_2 + M \rightarrow n\text{-}C_3F_7CF(OC_2H_4O_2\bullet)CF(CF_3)_2 + M \quad (2)$$

The loss of HFE-7500 and the formation of products were monitored by FTIR spectroscopy with an infrared path length of 27.4 m and a resolution of 0.25 cm^{-1}. Infrared spectra were derived from 32 coadded interferograms.

Two sets of experiments were performed. First, relative rate techniques were used to determine the rate constant for the reaction of Cl atoms with HFE-7500 and $n\text{-}C_3F_7CF(OC(O)H)CF(CF_3)_2$. Second, the products of the atmospheric oxidation of HFE-7500 were investigated by irradiating HFE-7500/Cl_2/O_2/N_2 mixtures.

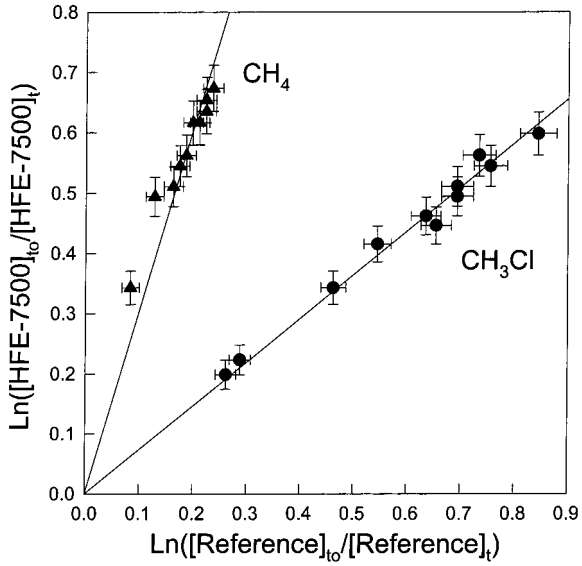

FIGURE 1. Decay of HFE-7500 versus CH_4 (▲) and CH3Cl (●) in the presence of OH radicals in 200 Torr of helium at 295 K.

Initial concentrations of the gas mixtures for the relative rate experiments of HFE-7500 were 1.7 mTorr of HFE-7500, 7−30 mTorr of the reference compounds [C_2H_5Cl or $CH_3OC(O)H$], and 100 mTorr of Cl_2 in 700 Torr of air diluent. In the study of the oxidation of HFE-7500, reaction mixtures consisted of 1.7 mTorr of HFE-7500, 9−100 mTorr of Cl_2 and 10−550 Torr of O_2 at a total pressure of 700 Torr in N_2 diluent. All experiments were performed at 295 K.

3. Results and Discussion

3.1. Relative Rate Study of the Reaction of OH with HFE-7500. The kinetics of reaction 1 were measured relative to reactions 11 and 12 by use of the experimental system at MIT.

$$OH + HFE\text{-}7500 \rightarrow products \quad (1)$$

$$OH + CH_4 \rightarrow products \quad (11)$$

$$OH + CH_3Cl \rightarrow products \quad (12)$$

Loss of HFE-7500 versus the reference compounds is shown in Figure 1. The error bars on the data points in Figure 1 represent the uncertainty associated with the analysis. Linear least-squares analysis of the data in Figure 1 gives $k_1/k_{11} = 2.96 \pm 0.34$ and $k_1/k_{12} = 0.73 \pm 0.05$. Using $k_{11} = (6.3 \pm 0.6) \times 10^{-15}$ and $k_{12} = (3.6 \pm 0.7) \times 10^{-14}$ cm^3 $molecule^{-1}$ s^{-1} (*12*), we derive $k_1 = (1.86 \pm 0.29) \times 10^{-14}$ and $(2.63 \pm 0.56) \times 10^{-14}$ cm^3 $molecule^{-1}$ s^{-1}. Within the experimental uncertainties, the values of k_1 derived from the two different reference compounds are indistinguishable.

Close examination of Figure 1 reveals that there is more data scatter evident in the experiments obtained with CH_4 as reference than in those experiments with CH_3Cl. The reason for the greater scatter in the CH_4 data lies in the fact that CH_4 is significantly less reactive than HFE-7500, while CH_3Cl has a reactivity comparable to that of HFE-7500. Hence, as seen from Figure 1, the fractional loss of CH_4 spans the range 8−21% while that of CH_3Cl spans the range 23−57%. It is difficult to measure an 8% loss of CH_4 with great precision and this probably goes some way to explain why the first data point in the CH_4 series lies above the regression line,

which has been forced to fit through the origin. Given the scatter in the CH_4 data discussed above, we choose to cite a final value for k_1 that is based upon the data obtained with CH_3Cl as reference. Hence, $k_1 = (2.6 \pm 0.6) \times 10^{-14}$ cm^3 molecule^{-1} s^{-1}; the quoted uncertainty includes statistical uncertainty in k_1/k_{12} and possible systematic errors associated with the uncertainty in k_{12}, and hence reflects the accuracy of the measurement of k_1.

This result can be compared to $k(OH + C_2H_5OC_2H_5) = 1.3 \times 10^{-11}$ (*13*), $k(OH + n\text{-}C_4F_9OC_2H_5) = (6.4 \pm 0.7) \times 10^{-14}$ (*5*), and $k(OH + (CF_3)_2CFCF_2OC_2H_5) = (7.7 \pm 0.8) \times 10^{-14}$ cm^3 molecule^{-1} s^{-1} (*5*). The 295-fold reduction in the reactivity of the OC_2H_5 group in HFE-7500 compared to that in diethyl ether presumably reflects the increase in C−H bond strength associated with the presence of multiple fluorinated substituents (*14*). As might be expected for such structurally similar molecules, the reactivities of OH radicals toward HFE-7500, $n\text{-}C_4F_9OC_2H_5$, and $(CF_3)_2CFCF_2OC_2H_5$ are broadly comparable. The somewhat lower reactivity of HFE-7500 compared to $n\text{-}C_4F_9OC_2H_5$ and $(CF_3)_2CFCF_2OC_2H_5$ probably reflects a somewhat greater C−H bond strength in HFE-7500.

The value of k_1 can be used to provide an estimate of the atmospheric lifetime of HFE-7500. Assuming an atmospheric lifetime for CH_3CCl_3 with respect to reaction with OH radicals of 5.7 years (*15*) and a rate constant for the $CH_3CCl_3 + OH$ reaction of 1.0×10^{-14} cm^3 molecule^{-1} s^{-1} (*12*) leads to an estimate of the atmospheric lifetime of HFE-7500 of $(1.0 \times 10^{-14}/2.6 \times 10^{-14}) \times 5.7 = 2.2$ years. The optimal temperature for such a scaling analysis is 277 K (*16*) (rather than 295 K used here) but we do not have any data for k_1 at 277 K. By analogy to other HFEs (*12*), the temperature dependence of reaction 1 is expected to be very similar to that for reaction of OH radicals with CH_3CCl_3. Hence, the use of 295 K rather than 277 K is not expected to have any material impact on the estimated atmospheric lifetime.

3.2. Relative Rate Study of the Reaction of Cl with HFE-7500. Prior to investigating the atmospheric fate of $n\text{-}C_3F_7CF(OC_2H_4O\bullet)CF(CF_3)_2$ radicals, relative rate experiments were performed with the FTIR system at Ford Motor Company to investigate the kinetics of reaction 10. The techniques used are described in detail elsewhere (*17*). Cl atoms were generated by photolysis of molecular chlorine:

$$Cl_2 + h\nu \rightarrow 2Cl \qquad (13)$$

$$Cl + n\text{-}C_3F_7CF(OC_2H_5)CF(CF_3)_2 \rightarrow n\text{-}C_3F_7CF(OC_2H_4\bullet)CF(CF_3)_2 + HCl \qquad (10)$$

The kinetics of reaction 10 were measured relative to the reactions of Cl atoms with ethyl chloride and methyl formate (reactions 14 and 15):

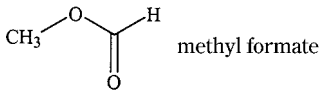

methyl formate

$$Cl + C_2H_5Cl \rightarrow \text{products} \qquad (14)$$

$$Cl + CH_3OC(O)H \rightarrow \text{products} \qquad (15)$$

Reaction mixtures consisted of 1.7−1.9 mTorr of HFE-7500, 100−110 mTorr of Cl_2, and 29 mTorr of C_2H_5Cl or 7−8 mTorr of $CH_3OC(O)H$ in 700 Torr of air diluent. The observed losses of HFE-7500 versus those of reference compounds are shown in Figure 2A. Linear least-squares analysis gives $k_{10}/k_{14} = 0.32 \pm 0.04$ and $k_{10}/k_{15} = 1.44 \pm 0.20$. Using $k_{14} = 8.04 \times 10^{-12}$ (*18*) and $k_{15} = 1.4 \times 10^{-12}$ (*19*) gives $k_{10} = (2.6 \pm 0.3) \times 10^{-12}$ and $k_{10} = (2.0 \pm 0.3) \times 10^{-12}$ cm^3 molecule^{-1} s^{-1}, respectively.

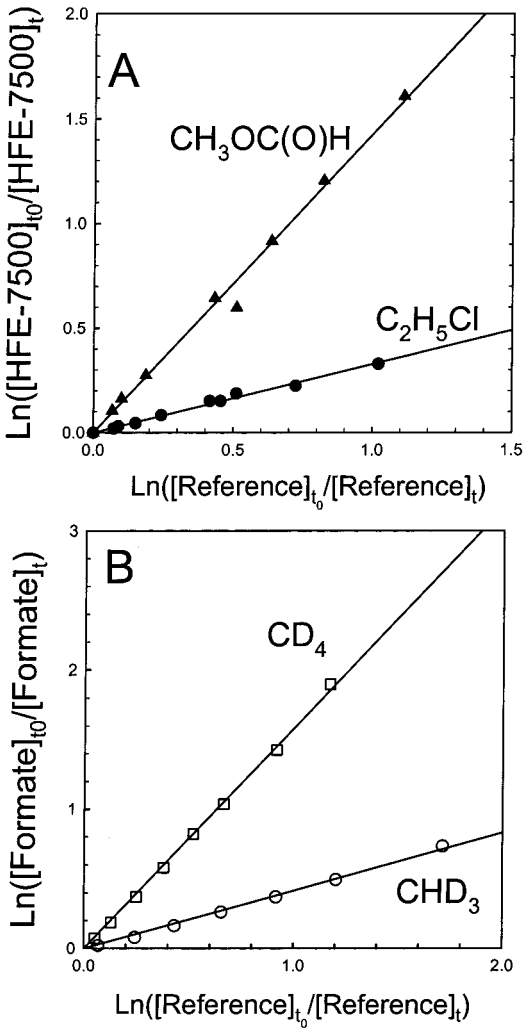

FIGURE 2. (A) Decay of HFE-7500 versus C_2H_5Cl (●) and $CH_3OC(O)H$ (▲) in the presence of Cl atoms in 700 Torr of N_2 at 295 K. (B) Decay of $n\text{-}C_3F_7CF(OCH_2CH_2O_2\bullet)CF(CF_3)_2$ versus CHD_3 (○) and CD_4 (□) in the presence of Cl atoms in 700 Torr of N_2 at 295 K.

We estimate that potential systematic errors associated with uncertainties in the reference rate constants could add an additional 10% uncertainty range for k_{10}. Propagating this additional uncertainty gives $k_{10} = (2.6 \pm 0.4) \times 10^{-12}$ and $k_{10} = (2.0 \pm 0.4) \times 10^{-12}$ cm^3 molecule^{-1} s^{-1}. We choose to cite a final value of k_{10} that is an average of those determined with the two different reference compounds, together with error limits that encompass the extremes of the individual determinations. Hence, $k_{10} = (2.3 \pm 0.7) \times 10^{-12}$ cm^3 molecule^{-1} s^{-1}.

This result can be compared to $k(Cl + C_2H_5OC_2H_5) = (3.6 \pm 0.3) \times 10^{-10}$ (*20*) and $k(Cl + n\text{-}C_4F_9OC_2H_5) = (2.7 \pm 0.6) \times 10^{-12}$ (*5*). As with OH radicals, the reactivity of Cl atoms toward the $\text{-}OC_2H_5$ group in HFE-7500 is substantially lower than that in diethyl ether. The magnitude of the decrease in reactivity for the Cl atom reactions is somewhat less than that for OH radicals (a factor of 78 compared to a factor of 295), reflecting the fact that Cl atoms are, in general, less discriminating than OH radicals in their reactions with organic compounds. The less discriminating nature of Cl atoms is also evidenced by the fact that, in contrast to the situation for OH radicals discussed in the previous section, there is no discernible difference between the reactivity of Cl atoms toward $n\text{-}C_4F_9OC_2H_5$ and HFE-7500. The average concentration of Cl atoms in the atmosphere is much lower [by a factor of approximately 1000 (*21*)] than that of OH

radicals and reaction with Cl atoms will not be a substantial atmospheric loss of HFE-7500.

Finally, we can use the rate constants for reactions of Cl atoms and OH radicals with HFE-7500 to test the empirical relationship $\log [k(OH + HFE)] = (0.74 \pm 0.07) \log [k(Cl + HFE)] - (4.4 \pm 0.9)$ proposed recently to estimate $k(OH + HFE)$ from $k(Cl + HFE)$ or vica versa (*22*). Substituting a value of $k_{10} = 2.3 \times 10^{-12}$ into the above expression leads to a prediction of $k_1 = 9.7 \times 10^{-14}$ cm^3 molecule^{-1} s^{-1}. This prediction is a factor of 3.7 greater than the measured value of $k_1 = (2.6 \pm 0.6) \times 10^{-14}$ cm^3 molecule^{-1} s^{-1}, which provides some measure of the uncertainties inherent in the empirical relationship.

3.3. Relative Rate Studies of the Reactions of Cl with *n*-$C_3F_7CF(OC(O)H)CF(CF_3)_2$ and n-$C_3F_7CF(OC(O)CH_3)CF(CF_3)_2$. As discussed in section 3.4, *n*-$C_3F_7CF(OC(O)H)CF(CF_3)_2$ and *n*-$C_3F_7CF(OC(O)CH_3)CF(CF_3)_2$ were readily generated in the Ford chamber by UV irradiation of gas mixtures of 2 mTorr of HFE-7500, 100−200 mTorr of Cl_2, and 6−7 Torr of O_2 in 700 Torr of N_2 diluent. After all (>97%) of the HFE-7500 was consumed, a reference compound was added and the UV irradiation was resumed:

$$n\text{-}C_3F_7CF(OC(O)H)CF(CF_3)_2 + Cl \rightarrow n\text{-}C_3F_7CF(OC(O)\bullet)CF(CF_3)_2 + HCl \quad (16)$$

$$n\text{-}C_3F_7CF(OC(O)CH_3)CF(CF_3)_2 + Cl \rightarrow n\text{-}C_3F_7CF(OC(O)CH_2\bullet)CF(CF_3)_2 + HCl \quad (17)$$

$$CHD_3 + Cl \rightarrow \text{products} \quad (18)$$

$$CD_4 + Cl \rightarrow \text{products} \quad (19)$$

The rate constants k_{16} and k_{17} were derived by observing the relative loss rates of *n*-$C_3F_7CF(OC(O)H)CF(CF_3)_2$, *n*-$C_3F_7CF(OC(O)CH_3)CF(CF_3)_2$, and the reference compounds. Figure 2b shows loss of *n*-$C_3F_7CF(OC(O)H)CF(CF_3)_2$ versus losses of reference compounds. Linear least-squares analysis of the data in Figure 2b gives $k_{16}/k_{18} = 0.42 \pm 0.04$ and $k_{16}/k_{19} = 1.58 \pm 0.12$. Using $k_{18} = 2.32 \times 10^{-14}$ (*17*) and $k_{19} = 6.1 \times 10^{-15}$ cm^3 molecule^{-1} s^{-1} (*17*), we derive $k_{16} = (9.7 \pm 0.9) \times 10^{-15}$ and $(9.6 \pm 0.5) \times 10^{-15}$ cm^3 molecule^{-1} s^{-1}. We estimate that potential systematic errors associated with uncertainties in the reference rate constants contribute an additional 10% uncertainty range for k_{15}. Propagating this additional uncertainty gives $k_{16} = (9.7 \pm 1.4) \times 10^{-15}$ and $(9.6 \pm 1.2) \times 10^{-15}$ cm^3 molecule^{-1} s^{-1}. We choose to cite a final value for k_{16} that is the average of those determined with the three different reference compounds, together with error limits that encompass the extremes of the individual determinations. Hence, $k_{16} = (9.7 \pm 1.4) \times 10^{-15}$ cm^3 molecule^{-1} s^{-1}, and the quoted uncertainty reflects the accuracy of the measurements. The rate constant k_{16} is 237 times lower than k_{10}. This is consistent with the behavior of other formates, which are typically significantly less reactive toward Cl atoms than the ethers from which they are derived [e.g., $k(Cl + CF_3OCH_3)/k(Cl + CF_3OC(O)H) = 143 \pm 27$ (*23*)].

During the present series of experiments no discernible loss (<2%) of *n*-$C_3F_7CF(OC(O)CH_3)CF(CF_3)_2$ was observed while consumptions of CHD_3 and CD_4 were 5−90%. From this observation we are able to derive an upper limit of $k_{17} < 6 \times 10^{-17}$ cm^3 molecule^{-1} s^{-1}.

3.4. Study of the Mechanism of the Atmospheric Oxidation of HFE-7500. The atmospheric degradation mechanism of HFE-7500 was studied by UV irradiation of HFE-7500/Cl_2/O_2/N_2 mixtures in the FTIR−smog chamber system at Ford. Experiments were performed at a constant total pressure of 700 Torr with the O_2 partial pressure varied over the range 10−700 Torr. The relative intensities of the infrared features of the products of the Cl atom initiated oxidation of HFE-7500 varied with the O_2 partial pressure. A careful comparison of the IR features formed in low and high [O_2] experiments revealed that two distinct products, or sets of products, were formed in the chamber. We will label these two products X and Y. Figure 3 shows IR spectra of HFE-7500, X, and Y. IR features attributable to X were observed at 984, 1133, 1139, 1167, 1257, 1304, and 1841 cm^{-1}. IR features attributable to Y were observed at 980, 1160, 1257, 1305, and 1812 cm^{-1}. The increases in X and Y scaled linearly with the loss of HFE-7500 over the range of HFE-7500 consumptions of 10−90%, suggesting the absence of significant secondary loss processes for X and Y. As shown in Figure 4, as the O_2 partial pressure was increased, the yield of Y decreased while that of X increased. For O_2 partial pressures greater than 400 Torr there was little change in the yields of X and Y.

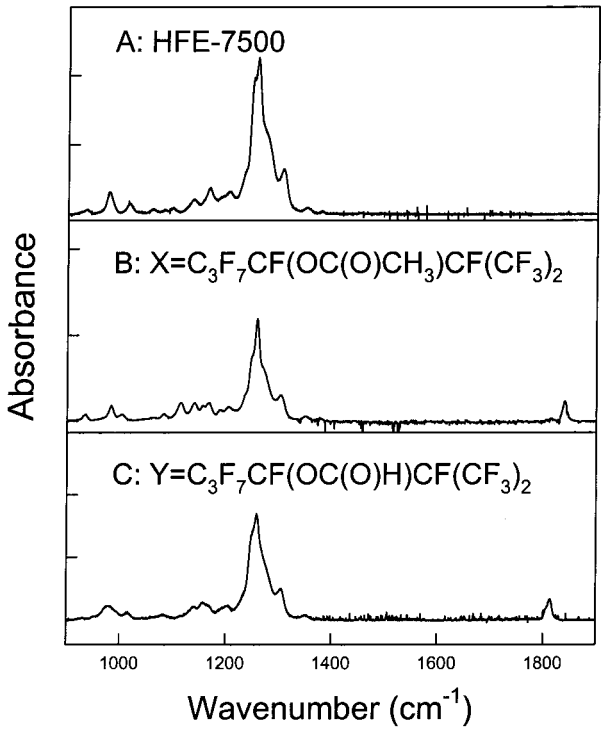

FIGURE 3. Infrared spectra of HFE-7500 (A), X = *n*-$C_3F_7CF(OC(O)CH_3)CF(CF_3)_2$ (B), and Y = *n*-$C_3F_7CF(OC(O)H)CF(CF_3)_2$ (C).

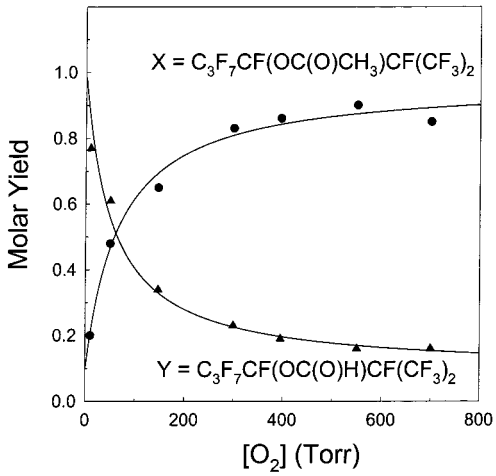

FIGURE 4. Observed yields of X = *n*-$C_3F_7CF(OC(O)CH_3)CF(CF_3)_2$ (●) and Y = *n*-$C_3F_7CF(OC(O)H)CF(CF_3)_2$ (▲) versus the O_2 partial pressure following the UV irradiation of HFE-7500/Cl_2/N_2/O_2 mixtures at 700 Torr total pressure and 295 K. The curves are fits to the data; see text for details.

The reaction of Cl atoms with HFE-7500 in the presence of O_2 gives rise to two different peroxy radicals, which in turn will undergo self- and cross-reaction to give the corresponding alkoxy radicals:

$$n\text{-}C_3F_7CF(OCHO_2\bullet CH_3)CF(CF_3)_2 + RO_2 \rightarrow n\text{-}C_3F_7CF(OCHO\bullet CH_3)CF(CF_3)_2 + RO + O_2 \quad (20a)$$

$$n\text{-}C_3F_7CF(OCH_2CH_2O_2\bullet)CF(CF_3)_2 + RO_2 \rightarrow n\text{-}C_3F_7CF(OCH_2CH_2O\bullet)CF(CF_3)_2 + RO + O_2 \quad (20b)$$

There are several possible fates of these alkoxy radicals. For n-$C_3F_7CF(OCHO\bullet CH_3)CF(CF_3)_2$ radicals, the possibilities are

$$n\text{-}C_3F_7CF(OCHO\bullet CH_3)CF(CF_3)_2 + M \rightarrow n\text{-}C_3F_7CF(OC(O)H)CF(CF_3)_2 + CH_3\bullet + M \quad (21)$$

$$n\text{-}C_3F_7CF(OCHO\bullet CH_3)CF(CF_3)_2 + M \rightarrow n\text{-}C_3F_7CF(OC(O)CH_3)CF(CF_3)_2 + H\bullet + M \quad (22)$$

$$n\text{-}C_3F_7CF(OCHO\bullet CH_3)CF(CF_3)_2 + O_2 \rightarrow n\text{-}C_3F_7CF(OC(O)CH_3)CF(CF_3)_2 + HO_2\bullet \quad (23)$$

while for n-$C_3F_7CF(OCH_2CH_2O\bullet)CF(CF_3)_2$ radicals the possibilities are

$$n\text{-}C_3F_7CF(OCH_2CH_2O\bullet)CF(CF_3)_2 + M \rightarrow n\text{-}C_3F_7CF(OCH_2\bullet)CF(CF_3)_2 + HCHO + M \quad (24)$$

$$n\text{-}C_3F_7CF(OCH_2CH_2O\bullet)CF(CF_3)_2 + M \rightarrow n\text{-}C_3F_7CF(OCH_2C(O)H)CF(CF_3)_2 + H\bullet + M \quad (25)$$

$$n\text{-}C_3F_7CF(OCH_2CH_2O\bullet)CF(CF_3)_2 + O_2 \rightarrow n\text{-}C_3F_7CF(OCH_2C(O)H)CF(CF_3)_2 + HO_2\bullet \quad (26)$$

The increase in the yield of X and decrease in Y with increasing $[O_2]$ shows that reactions 23 and/or 26 become important at high $[O_2]$. The unknown X is either n-$C_3F_7CF(OC(O)CH_3)CF(CF_3)_2$, n-$C_3F_7CF(OCH_2C(O)H)CF(CF_3)_2$, or both. There are four aspects of the IR spectrum which suggest that X is the acetate n-$C_3F_7CF(OC(O)CH_3)CF(CF_3)_2$. First, the observed carbonyl stretching frequency of 1841 cm^{-1} is typical for a fluorinated ester (*4*−*6*). Second, there is no aldehydic C−H stretching feature in the 2720−2820 cm^{-1} region. Third, there is no significant -CH_2- scissors feature at approximately 1450 cm^{-1}. Finally, there is no -C(O)H deformation band at approximately 1400 cm^{-1}. The kinetic behavior of X is also consistent with its assignment as n-$C_3F_7CF(OC(O)CH_3)CF(CF_3)_2$ rather than n-$C_3F_7CF(OCH_2C(O)H)CF(CF_3)_2$. Aldehydes react rapidly with Cl atoms with rate constants of typically 10^{-11}−10^{-10} cm^3 $molecule^{-1}$ s^{-1} (*12*). In contrast, esters are relatively unreactive toward Cl atoms; for example, $k(Cl + CH_3C(O)OCH_3) = 2.2 \times 10^{-12}$ cm^3 $molecule^{-1}$ s^{-1} with more than 95% of the reaction occurring at the -OCH_3 site (*24*). It was determined in the present work (see section 3.3) that Cl atoms are relatively unreactive toward X (rate constant $< 6 \times 10^{-17}$ cm^3 $molecule^{-1}$ s^{-1}); thus the kinetic behavior of X is consistent with its identification as n-$C_3F_7CF(OC(O)CH_3)CF(CF_3)_2$. In the following we will proceed on the assumption that X is the acetate n-$C_3F_7CF(OC(O)CH_3)CF(CF_3)_2$.

As noted above and illustrated in Figure 4, increase in the O_2 partial pressure led to an increase in the yield of product X and a corresponding decrease in the yield of product Y. The simplest explanation of this observation is that product Y is the formate n-$C_3F_7CF(OC(O)H)CF(CF_3)_2$ formed via reaction 21, which is in competition with the O_2-dependent reaction 23. The observed dependence of the yields of the formate and acetate on $[O_2]$ then reflects a competition between reactions 21 and 23. For clarity the reactions leading to X and Y are shown schematically in Figure 5.

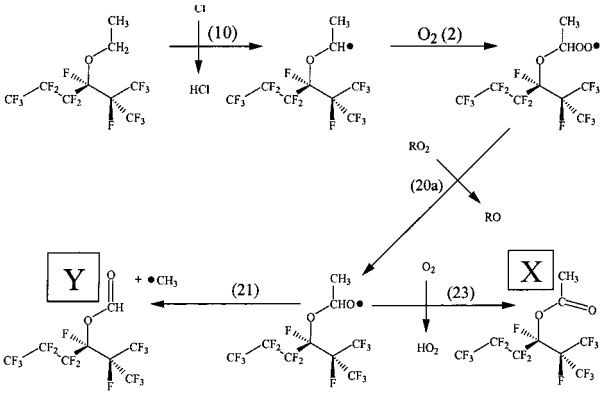

FIGURE 5. Schematic depiction of the reactions discussed in section 3.4 leading to formation of X and Y. Reaction numbers are given in parentheses.

As shown in Figure 4, while the yield of n-$C_3F_7CF(OC(O)H)CF(CF_3)_2$ decreases as the O_2 partial pressure is increased from 3 to 400 Torr, further increase in $[O_2]$ has little or no effect and the n-$C_3F_7CF(OC(O)H)CF(CF_3)_2$ yield remains at approximately 20%. This behavior suggests that there is a source of n-$C_3F_7CF(OC(O)H)CF(CF_3)_2$ which is independent of $[O_2]$. A likely source for this n-$C_3F_7CF(OC(O)H)CF(CF_3)_2$ is the n-$C_3F_7CF(OCH_2CH_2O\bullet)CF(CF_3)_2$ alkoxy radical. There are three possible fates of the n-$C_3F_7CF(OCH_2CH_2O\bullet)CF(CF_3)_2$ radical: reactions 24−26. Decomposition via reaction 24 gives the carbon-centered radical n-$C_3F_7CF(OCH_2\bullet)CF(CF_3)_2$. By analogy to the behavior of analogous radicals [e.g., $CF_3OCH_2\bullet$ (*23*), $C_2F_5OCH_2\bullet$ (*25*), $C_3F_7OCH_2\bullet$ (*6*), and $(CF_3)_2CFCF_2OCH_2\bullet$ (*4*)] the $C_3F_7CF(OCH_2\bullet)CF(CF_3)_2$ radical is expected to react to give the formate, $C_3F_7CF(OC(O)H)CF(CF_3)_2$. Reactions 25 and 26 produce $C_3F_7CF(OCH_2C(O)H)CF(CF_3)_2$, which contains an aldehydic functional group and, as discussed above, is expected to be at least 1 order of magnitude more reactive than HFE-7500 toward Cl atoms and will be converted into n-$C_3F_7CF(OCH_2\bullet)CF(CF_3)_2$ radicals and hence into n-$C_3F_7CF(OC(O)H)CF(CF_3)_2$ via reactions 27−30. There were no IR product features that could be ascribed to the aldehyde $C_3F_7CF(OCH_2C(O)H)CF(CF_3)_2$ in the system, but this does not preclude its formation and subsequent loss via reaction 27:

$$n\text{-}C_3F_7CF(OCH_2C(O)H)CF(CF_3)_2 + Cl \rightarrow n\text{-}C_3F_7CF(OCH_2C(O)\bullet)CF(CF_3)_2 + HCl \quad (27)$$

$$n\text{-}C_3F_7CF(OCH_2C(O)\bullet)CF(CF_3)_2 + O_2 + M \rightarrow n\text{-}C_3F_7CF(OCH_2C(O)OO\bullet)CF(CF_3)_2 + M \quad (28)$$

$$n\text{-}C_3F_7CF(OCH_2C(O)OO\bullet)CF(CF_3)_2 + RO_2 \rightarrow n\text{-}C_3F_7CF(OCH_2C(O)O\bullet)CF(CF_3)_2 + RO + O_2 \quad (29)$$

$$n\text{-}C_3F_7CF(OCH_2C(O)O\bullet)CF(CF_3)_2 + M \rightarrow n\text{-}C_3F_7CF(OCH_2\bullet)CF(CF_3)_2 + CO_2 + M \quad (30)$$

The decrease in the yield of n-$C_3F_7CF(OC(O)H)CF(CF_3)_2$ and increase of n-$C_3F_7CF(OC(O)CH_3)CF(CF_3)_2$ with increasing $[O_2]$ shown in Figure 4 reflects a competition between reactions 21 and 23 for the available n-$C_3F_7CF(OCHO\bullet CH_3)CF(CF_3)_2$ radicals. We can place the yield of n-$C_3F_7CF(OC(O)CH_3)CF(CF_3)_2$ on an absolute basis by equating the increase in its yield to the *decrease* in the yield of n-$C_3F_7CF(OC(O)H)CF(CF_3)_2$ and by assuming that these two species account for all of the observed loss of HFE-7500. It was on this basis that the n-$C_3F_7CF(OC(O)CH_3)CF(CF_3)_2$ and n-C_3F_7-

$CF(OC(O)H)CF(CF_3)_2$ yields in Figure 4 were calibrated. The dependence of the product yields in Figure 4 on $[O_2]$ can be used to extract a value for the rate constant ratio k_{23}/k_{21}. Assuming that the fate of n-$C_3F_7CF(OCHO\bullet CH_3)CF(CF_3)_2$ radicals is either unimolecular decomposition via reaction 21 or bimolecular reaction with O_2 (reaction 23) and that all n-$C_3F_7CF(OCH_2CH_2O\bullet)CF(CF_3)_2$ radicals are converted into n-$C_3F_7CF(OC(O)H)CF(CF_3)_2$, then the yield of n-$C_3F_7CF(OC(O)H)CF(CF_3)_2$ can be related to the molar yields of the two alkoxy radicals and the rate constant ratio k_{23}/k_{21}:

$$Y[n\text{-}C_3F_7CF(OC(O)H)CF(CF_3)_2] = Y[n\text{-}C_3F_7CF(OCHO\bullet CH_3)CF(CF_3)_2]\left[\frac{1}{(k_{23}/k_{21})[O_2]+1}\right] + Y[n\text{-}C_3F_7CF(OCH_2CH_2O\bullet)CF(CF_3)_2] \quad \text{(I)}$$

while the yield of n-$C_3F_7CF(OC(O)CH_3)CF(CF_3)$ is given by

$$Y[n\text{-}C_3F_7CF(OC(O)CH_3)CF(CF_3)] = Y[n\text{-}C_3F_7CF(OCHO\bullet CH_3)CF(CF_3)_2]\left[\frac{(k_{23}/k_{21})[O_2]}{(k_{23}/k_{21})[O_2]+1}\right] + C \quad \text{(II)}$$

The term C in expression II was added to account for the nonzero intercept in the n-$C_3F_7CF(OC(O)CH_3)CF(CF_3)$ yield plot and is discussed later. The curves in Figure 4 are fits of the above expressions to the experimental data. A least-squares fit to the n-$C_3F_7CF(OC(O)H)CF(CF_3)_2$ data gives $Y[n\text{-}C_3F_7CF(OCHO\bullet CH_3)CF(CF_3)_2] = 0.91 \pm 0.05$, $Y[n\text{-}C_3F_7CF(OCH_2CH_2O\bullet)CF(CF_3)_2] = 0.04 \pm 0.03$, and $k_{23}/k_{21} = 0.011 \pm 0.002$ Torr^{-1}, while a fit to the n-$C_3F_7CF(OC(O)CH_3)CF(CF_3)$ data gives $Y[n\text{-}C_3F_7CF(OCHO\bullet CH_3)CF(CF_3)_2] = 0.88 \pm 0.07$, $k_{23}/k_{21} = 0.015 \pm 0.004$ Torr^{-1}, and $C = 0.09 \pm 0.06$. It is gratifying to note that least-squares fits of expressions I and II to the variation of the yields of n-$C_3F_7CF(OC(O)H)CF(CF_3)_2$ and n-$C_3F_7CF(OC(O)CH_3)CF(CF_3)$ with $[O_2]$ give indistinguishable values of k_{23}/k_{21}. We choose to quote a final value of k_{23}/k_{21} that is an average of the two determinations, with error limits that encompass the extremes of the individual determinations; $k_{23}/k_{21} = 0.013 \pm 0.006$ Torr^{-1}. In 1 atm of air at 295 K, the O_2 partial pressure is 160 Torr and 68% of the n-$C_3F_7CF(OCHO\bullet CH_3)CF(CF_3)_2$ radicals will react with O_2 while the remainder will decompose via reaction 21. In the atmosphere most of the oxidation of HFE-7500 will occur at elevated altitudes and hence temperatures and total pressures below that employed here. Lower temperature favors reaction 23, while lower total pressure (and hence O_2 partial pressure) favors reaction 21. Reaction 21 is a unimolecular decomposition reaction and will have a substantial activation barrier. As with other similar competitions [e.g., in the case of the $CF_3CFHO\bullet$ radical (*8*)], it is expected that the temperature effect will greatly dominate the pressure effect and that the atmospheric fate of n-$C_3F_7CF(OCHO\bullet CH_3)CF(CF_3)_2$ radicals will be dominated by reaction with O_2.

At this point we need to return to the inclusion of factor C in expression II. It is apparent from Figure 4 that n-$C_3F_7CF(OC(O)CH_3)CF(CF_3)$ has a nonzero y-axis intercept. There are several possible causes of this intercept: (i) reaction 21 is important, (ii) there is a contribution due to a molecular channel of the peroxy radical self- and cross-reactions which gives the ester, or (iii) the ester is formed in the n-$C_3F_7CF(OCHO_2\bullet CH_3)CF(CF_3)_2 + HO_2$ reaction. We are not able to distinguish between these possibilities at the present time. It should be noted that the important conclusion from this study, namely, that the atmospheric fate of n-$C_3F_7CF(OCHO\bullet CH_3)CF(CF_3)_2$ radicals is dominated by reaction with O_2, is insensitive to the cause of the intercept. To quantify the effect of factor C on the value of k_{23}/k_{21} obtained in the analysis, a modified version of expression II (without C) was fitted to the data in Figure 4. Omission of C leads to a value $k_{23}/k_{21} = 0.021 \pm 0.007$ Torr^{-1}, which is not substantially different from the value of $k_{23}/k_{21} = 0.015 \pm 0.004$ Torr^{-1} obtained from the complete expression II. Finally, we note that factor C does not need to be incorporated into expression I as the factor $Y[n\text{-}C_3F_7CF(OCH_2CH_2O\bullet)CF(CF_3)_2]$ serves to account for the fact that there appears to be a non-O_2-dependent source of the formate Y.

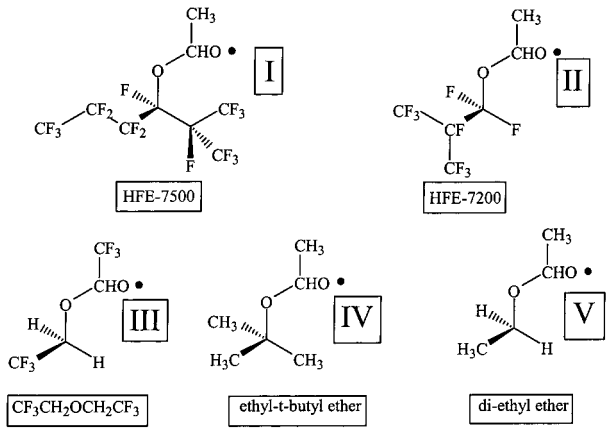

FIGURE 6. Secondary alkoxy radicals derived from HFE-7500 (I), $(CF_3)_2CFCF_2OC_2H_5$ (main component of HFE-7200) (II), bis(2,2,2-trifluoroethyl) ether (III), ethyl *tert*-butyl ether (IV), and diethyl ether (V).

In section 3.2 it was concluded that the atmospheric fate of HFE-7500 is reaction with OH radicals and that reaction with Cl atoms is of little atmospheric significance. This raises the question, "Of what help is a study of the products of Cl atom-initiated oxidation of HFE-7500 to understanding the products of the OH radical-initiated oxidation?" To answer this question we need to consider two pieces of information. First, the molar yield of n-$C_3F_7CF(OCHO\bullet CH_3)CF(CF_3)_2$ radicals derived from the data in Figure 4 is approximately 0.90, indicating that the majority of the reaction of Cl atoms with HFE-7500 occurs at the -CH_2- site. Second, as evident from sections 3.1 and 3.2, OH radicals are less reactive and more discriminating than Cl atoms. It is likely that >90% of the reaction of OH radicals with HFE-7500 occurs at the -CH_2- site and that Cl atoms provide a good surrogate for OH radicals in understanding the mechanism of the atmospheric oxidation of HFE-7500.

4. Implications for Atmospheric Chemistry

4.1. Atmospheric Fate of Alkoxy Radicals of the General Formula $ROCH(O\bullet)CH_3$. As discussed in section 3.4, two competing loss processes were identified for n-$C_3F_7CF(OCHO\bullet CH_3)CF(CF_3)_2$ radicals: reaction with O_2 and decomposition ($k_{23}/k_{21} = k_{O_2}/k_{diss} = 0.013 \pm 0.006$ Torr^{-1}). We can compare this behavior with the literature data for that of structurally similar secondary alkoxy radicals formed during the oxidation of HFE-7200 (**II**), $CF_3CH_2OCH_2CF_3$ (**III**), ethyl *tert*-butyl ether (**IV**), and diethyl ether (**V**): see Figure 6. In 1 atm of air at 295 K, reaction with O_2 and decomposition are competing loss processes for alkoxy radicals derived from HFE-7200 (**II**) with $k_{O_2}/k_{diss} = 0.026 \pm 0.010$ Torr^{-1} (*5*). In contrast, decomposition via C−C bond scission is the sole fate of the alkoxy radicals (**III**) (*26*), (**IV**) (*27*), and (**V**) (*27*). Given the obvious structural similarity of species **I** and **II** evident in Figure 6, it is not too surprising that they have indistinguishable values of k_{O_2}/k_{diss}. Comparing the chemistry of species **I** and **II** with those of **IV** and **V**, it is evident that fluorination of the R moiety in $ROCH(O\bullet)CH_3$ radicals leads to an increase in the relative importance of the reaction with O_2.

It is of interest to contrast the atmospheric fate of $ROCH(O\bullet)CH_3$ radicals derived from ethers to the atmospheric fate of $RCH(O\bullet)CH_3$ radicals derived from alkanes. At room temperature, $RCH(O\bullet)CH_3$ radicals react with O_2 with a rate constant of $k_{O_2} = 7.5 \times 10^{-15}$ cm^3 molecule^{-1} s^{-1} and undergo decomposition into $RCHO + CH_3\bullet$ with a rate constant of $k_{diss} = 28$ s^{-1} (*28*, *29*). In 1 atm of air, $k_{O_2}[O_2]/k_{diss} = 1400$. In contrast to the fate of $ROCH(O\bullet)CH_3$ radicals, the atmospheric fate of $RCH(O\bullet)CH_3$ radicals is completely dominated by reaction with O_2. It can be concluded that the ether functionality in $ROCH(O\bullet)CH_3$ radicals either decreases the rate of O_2 reaction or increases the rate of the C−C bond scission, or both. Introduction of the ether functionality will change the bond strengths in the radical. The decomposition channel will be more sensitive than the O_2 reaction to changes in chemical bond strength. The simplest explanation for the different behavior of $ROCH(O\bullet)CH_3$ and $RCH(O\bullet)CH_3$ radicals is that the presence of the ether functionality decreases the $C-CH_3$ bond strength, thereby facilitating the decomposition channel. High level ab initio calculations are needed to provide further insight into the fundamental cause of the different behavior of the two types of alkoxy radical. Such calculations are beyond the scope of the present work.

4.2. Atmospheric Chemistry and Environmental Impact of HFE-7500. We present herein a large body of kinetic and mechanistic data pertaining to the atmospheric chemistry of HFE-7500. The atmospheric lifetime of HFE-7500 is determined by its reaction with OH radicals and is estimated to be 2.2 years. The atmospheric oxidation of HFE-7500 gives a fluorinated acetate, n-$C_3F_7CF(OC(O)CH_3)CF(CF_3)_2$, and a fluorinated formate, n-$C_3F_7CF(OC(O)H)CF(CF_3)_2$. The atmospheric fate of these two esters will probably be hydrolysis, which will produce n-$C_3F_7CF(OH)CF(CF_3)_2$ and $CH_3C(O)OH$, and n-$C_3F_7CF(OH)CF(CF_3)_2$ and $HC(O)OH$. Acetic acid and formic acid are ubiquitous naturally occurring compounds in the atmosphere and the additional burden associated with the oxidation of HFE-7500 is of no consequence. In contrast, n-$C_3F_7CF(OH)CF(CF_3)_2$ is not a naturally occurring compound. By analogy with the well-known behavior of CF_3OH, we expect that the fluorinated alcohol n-$C_3F_7CF(OH)CF(CF_3)_2$ will undergo heterogeneous decomposition to give $HF + n$-$C_3F_7C(O)CF(CF_3)_2$. The perfluoroketone n-$C_3F_7C(O)CF(CF_3)_2$ will not react with OH radicals, NO_3 radicals, or ozone. While there are no available data concerning the rate of photolysis or hydrolysis of n-$C_3F_7C(O)CF(CF_3)_2$, such data exist for hexafluoroacetone. Hexafluoroacetone (CF_3COCF_3) is believed to be removed from the atmosphere via both photolysis and hydrolysis on a time scale of 5−10 days (*30*). It is likely that a similar fate awaits n-$C_3F_7C(O)CF(CF_3)_2$; further work is needed to clarify the atmospheric fate of this compound.

With regard to the environmental impact of HFE-7500 we can make the following three statements. First, HFE-7500 does not contain any chlorine and will not contribute to stratospheric ozone depletion via the well-established chlorine based chemistry. As with all hydrofluorocarbons (HFCs) and hydrofluoroethers (HFEs) the ozone depletion potential of HFE-7500 is zero. Second, the atmospheric lifetime of HFE-7500 is approximately 2.2 years. Using the method of Pinnock et al. (*31*) and the IR spectra of HFE-7500 shown in Figure 3A and CFC-11 reported elsewhere (*6*), we calculate instantaneous forcings for HFE-7500 and CFC-11 of 0.37 W/m^2 and 0.26 W/m^2, respectively. Values of the GWP (global warming potential) for HFE-7500 (relative to CFC-11) can then be estimated (*32*):

$$GWP_{HFE-7500} = \left(\frac{IF_{HFE-7500}}{IF_{CFC-11}}\right)\left(\frac{\tau_{HFE-7500}M_{CFC-11}}{\tau_{CFC-11}M_{HFE-7500}}\right)\left(\frac{1-\exp(-t/\tau_{HFE-7500})}{1-\exp(-t/\tau_{CFC-11})}\right)$$

where $IF_{HFE-7500}$, IF_{CFC-11}, $M_{HFE-7500}$, M_{CFC-11}, $\tau_{HFE-7500}$, and τ_{CFC-11} are the instantaneous forcings, molecular weights, and atmospheric lifetimes of the two species and t is the time horizon over which the forcing is integrated. Using $\tau_{HFE-7500} = 2.2$ years and $\tau_{CFC-11} = 50$ years (*31*), we estimate that the GWP of HFE-7500 is ≈0.06 for a 20-year horizon and ≈0.02 for a 100-year time horizon. Because of its short atmospheric lifetime, HFE-7500 has a small GWP. Emission of HFE-7500 into the atmosphere will not contribute significantly to radiative forcing of global climate change. Third, the atmospheric oxidation of HFE-7500 will produce a fluorinated acetate, n-$C_3F_7CF(OC(O)CH_3)CF(CF_3)_2$, and a fluorinated formate, n-$C_3F_7CF(OC(O)H)CF(CF_3)_2$, neither of which is expected to be persistent or pose any significant environmental hazard.

Acknowledgments

We thank John Owens (3M Specialty Materials) for supplying the samples of HFE-7500 used in this work, Roc Carter (Ford) for help in interpretation of IR spectra, 3M Specialty Materials for funding the work performed at MIT, and the Japanese Government for a NEDO grant and a Monbusho science grant for the priority field "Radical Reactions" which made this collaborative research project possible.

Literature Cited

(1) Molina, M. J.; Rowland, F. S. *Nature* **1974**, *249*, 810.
(2) Farman, J. D.; Gardiner, B. G.; Shanklin, J. D. *Nature* **1985**, *315*, 207.
(3) J. Owens, 3M Specialty Materials, private communication, 1999.
(4) Wallington, T. J.; Schneider, W. F.; Sehested, J.; Bilde, M.; Platz, J.; Nielsen, O. J.; Christensen, L. K.; Molina, M. J.; Molina, L. T.; Wooldridge, P. W. *J. Phys. Chem. A.* **1997**, *101*, 8264.
(5) Christensen L. K.; Sehested, J.; Nielsen, O. J.; Bilde, M.; Wallington, T. J.; Guschin, A.; Molina, L. T.; Molina, M. J. *J. Phys. Chem. A* **1998**, *102*, 4839.
(6) Ninomiya, Y.; Kawasaki, M.; Guschin, A.; Molina, L. T.; Molina, M.; Wallington, T. J. *Environ. Sci. Technol.* **2000**, *34*, 2973.
(7) 3M Technical Information Sheet 2001.
(8) Wallington, T. J.; Schneider, W. F.; Worsnop, D. R.; Nielsen, O. J.; Sehested, J.; Debruyn, W. J.; Shorter, J. A. *Environ. Sci. Technol.* **1994**, *28*, 320.
(9) Tyndall, G. S.; Cox, R. A.; Grainer, C.; Lesclaux, R.; Moortgat, G. K.; Pilling, M. J.; Ravishankara, A. R.; Wallington, T. J. *J. Geophys. Res.* **2001**, *106*, 12157.
(10) Tang, Y. Atmospheric Fate of Various Fluorocarbons. MS Thesis, Massachusetts Institute of Technology, Cambridge, MA, 1993.
(11) Wallington, T. J.; Japar, S. M. *J. Atmos. Chem.* **1989**, *9*, 399.
(12) DeMore W. B.; Sander, S. P.; Golden, D. M.; Hampson, R. F.; Kurylo, M. J.; Howard, C. J.; Ravishankara, A. R.; Kolb, C. E.; Molina, M. J. JPL Publication No. 94-26; NASA Jet Propulsion Lab: Pasadena, CA, 1997.
(13) Atkinson, R. *J. Phys. Chem. Ref. Data. Monogr. 2*, **1994**.
(14) Stein, S. E.; Rukkers, J. M.; Brown, R. L. NIST Standard Reference Database 25: Structures and Properties; NIST: Gaithersburg, MD, 1991.
(15) Prinn, R. G.; Weiss, R. F.; Miller, B. R.; Huang, J.; Alyea, F. N.; Cunnold, D. M.; Fraser, P. J.; Hartley, D. E.; Simmonds, P. G. *Science* **1995**, *269*, 187.
(16) Spivakovsky, C. M.; Logan, J. A.; Montzka, S. A.; Balkanski, Y. L.; Foreman-Fowler, M.; Jones, D. B. A.; Horowitz, L. W.; Fusco, A. C.; Brenninkmeijer, C. A. M.; Prather, M. J.; Wofsy, S. C.; McElroy, M. B. *J. Geophys. Res.* **2000**, *105*, 8931.
(17) Wallington, T. J.; Hurley, M. D. *Chem. Phys. Lett.* **1992**, *189*, 437.
(18) Wine, P. H.; Semmes, D. H. *J. Phys. Chem.* **1983**, *87*, 3572.
(19) Wallington, T. J.; Hurley, M. D.; Ball, J. C.; Jenkin, M. E. *Chem. Phys. Lett.* **1993**, *211*, 41.
(20) Wallington, T. J.; Skewes, L. M.; Siegl, W. O.; Wu, C.-H.; Japar, S. M. *Int. J. Chem. Kinet.* **1988**, *20*, 867.
(21) Wingenter, O. W.; Blake, D. R.; Blake, N. J.; Sive, B. C.; Rowland, F. S.; Atlas, E.; Flocke, F. *J. Geophys. Res.* **1999**, *104*, 21819.
(22) Goto, M.; Kawasaki, M.; Wallington, T. J.; Hurley, M. D.; Sharratt, A. P. *Int. J. Chem. Kinet.* **2002**, *34*, 139.

(23) Christensen, L. K.; Wallington, T. J.; Guschin, A.; Hurley, M. D. *J. Phys. Chem. A* **1999**, *103*, 4202.
(24) Christensen, L. K.; Ball, J. C.; Wallington, T. J. *J. Phys. Chem. A.* **2000**, *104*, 345.
(25) Nohara, K.; Toma, M.; Kutsuna, S.; Takeuchi, K.; Ibusuki, T. *Environ. Sci. Technol*. **2001**, *35*, 114.
(26) Wallington, T. J.; Guschin, A.; Stein, T. N. N.; Platz, J.; Sehested, J.; Christensen, L. K.; Nielsen, O. J. *J. Phys. Chem. A* **1998**, *102*, 1152.
(27) Japar, S. M.; Wallington, T. J.; Richert, J. F. O.; Ball, J. C. *Int. J. Chem. Kinet*. **1990**, *22*, 1257.
(28) Atkinson, R. *Atmos. Environ*. **1990**, *24A*, 1.
(29) Atkinson, R.; Baulch, D. L.; Cox, R. A.; Hampson, R. F., Jr.; Kerr, J. A.; Rossi, M. J.; Troe, J. *J. Phys. Chem. Ref. Data* **1999**, *28*, 191.
(30) Møgelberg, T. E.; Platz, J.; Nielsen, O. J.; Sehested, J.; Wallington, T. J. *J. Phys. Chem.* **1995**, *99*, 5373.
(31) Pinnock, S.; Hurley, M. D.; Shine, K. P.; Wallington, T. J.; Smyth, T. J. *J. Geophys. Res.* **1995,** *100*, 23227.
(32) Houghton, J. T.; Meira Filho, L. G.; Bruce, J.; Lee, H.; Callander, B. A.; Haites, E.; Harris, N.; Maskell, K. In *Climate Change 1994: Radiative Forcing of Climate Change and an evaluation of the IPCC IS92 Emission Scenarios*; Houghton, J. T., Ed.; Cambridge University Press: Cambridge, U.K., 1995; p 222 (Report of Working Groups I and III of the Intergovernmental Panel on climate change).

Received for review October 23, 2001. Revised manuscript received March 6, 2002. Accepted March 12, 2002.

ES0113798